CM 9071

NANYANG TECHNOLOGICAL UNIVERSITY

DIVISION OF CHEMISTRY AND BIOLOGICAL CHEMISTRY
SCHOOL OF PHYSICAL & MATHEMATICAL SCIENCES

Metal-Metal Bond Fluxionality in Phosphine-substituted Ru_3Sb_2 Organometallic Clusters

Submitted by: Liu Yang

U1140952C

Supervisor: Assoc Prof Leong Weng Kee

Academic Year: 2012/2013 Semester 2

Contents

1 Acknowledgement

I would like to express my sincere gratitude to my supervisor A/P Leong Weng Kee for providing me the opportunity to do my very first research project, as well as for his invaluable guidance on the project work and helpful suggestions on report-writing techniques.

I would also like to thank my mentor Li Yingzhou for his great effort contributed to educate me on various laboratory practices, as well as his support, motivation and inspiring suggestions throughout the project.

I would also like to gratefully acknowledge Dr. Rakesh Ganguly and Dr. Derek Ong for their assistance in performing the variable-temperature NMR experiments, and to thank all my lab mates: Liu Yu, Kumaran, Zhiyong, Bo Yang, Joey, Jingwei, Yuqian, Yongjia for their kindness and assistance during the last two months.

2 Abstract

This report investigates the fluxionality of phosphine-substitued Ru_3Sb_2 clusters. Three such clusters were synthesized and their fluxionality behaviors examined by variable-temperature NMR. The PMe_3-substituted species were found to have no fluxionality while the $PMePh_2$- and PPh_3-substituted ones showed evident coalescence of peaks in their corresponding VT-NMR spectra. Several kinetic parameters of the fluxional processes were also estimated to assist investigation of mechanisms.

3 Introduction

Previous studies have shown that five-membered osmium-antimony clusters exhibit molecular fluxionality via interchange of metal-metal bonds, accompanied by migration of one carbonyl ligand from one metal center to another by way of bridge-terminal exchange.[1] More recently, it has been found that the ruthenium analogue exhibited similar but even more rapid fluxionality (Scheme 1), and preliminary results suggested that a phoshine-substituted analogue may also exhibit similar behaviour.[2]

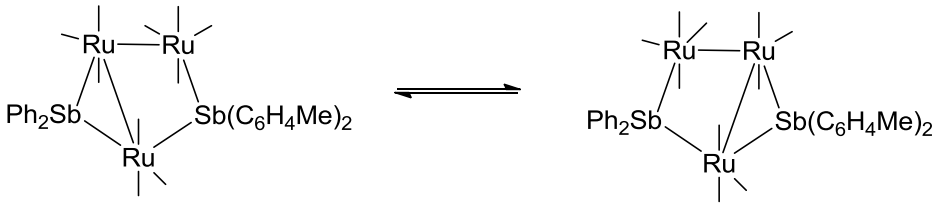

* Short bonds denote CO ligands

Scheme 1

It became of interest to examine the rate of exchange in these phosphine-substituted ruthenium-antimony clusters and if the nature of the phosphine has any effect on the fluxionality. Both ^{1}H and ^{31}P variable-temperature NMR can be utilized to study this dynamic process, provided that a proper "probe" was integrated into the molecule, such as a methyl or

p-tolyl group. Based on this premise, several phosphine-containing analogues, **1**, **2** and **3**, were planned and synthesized (Scheme 2).

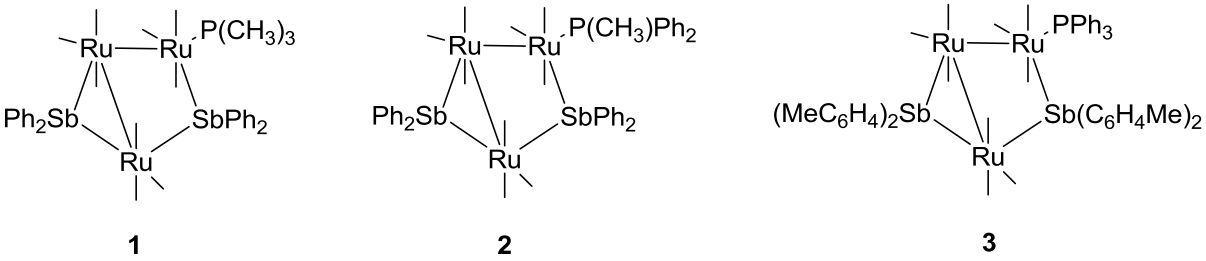

1 **2** **3**

Scheme 2

Various mechanisms can be employed to explain the fluxional behavior of such clusters, the most common one being the metal-metal bond interchange accompanied by concerted migration of a carbonyl ligand. A similar mechanism involving migration of the phosphine ligand has also been reported.[3] Besides, a "turnstile" rotation, where three facial ligands exchange positions by rotation around the normal line intersecting the center of the triangular face, is viable as well.[4]

4 Results and Discussion

*4.1 Synthesis of phosphine-substituted ruthenium-antimony clusters **1**, **2** and **3***

The unsubstituted ruthenium-antimony clusters $Ru_3(CO)_{10}(\mu\text{-}SbAr_2)_2$ (Ar = Ph or p-tolyl) were prepared by reacting $Ru_3(CO)_{12}$ with Sb_2Ph_4 or $Sb_2(tolyl)_4$. The distibine ligands were synthesized through the following reaction; this is more convenient than the reported method via sodium reduction of $SbAr_2Cl$ in liquid ammonia.[5]

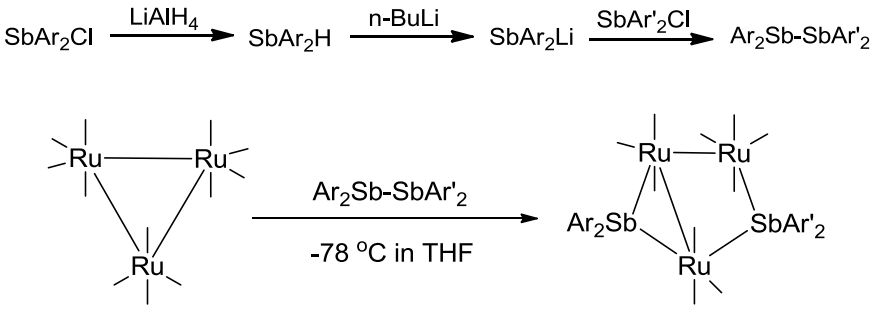

Scheme 3

The reaction can also be used to prepare unsymmetrically substituted distibines, however, in an attempt at this, transmetallation of the lithium salt with $SbAr'_2Cl$ was observed, leading to a mixture of homo- and cross-coupling products. A possible way to circumvent this is to use the diarylantimony chloride species that would produce the more stable lithium-antimony compound as the starting material to prevent transmetallation. For example, in the synthesis of $Sb_2(tolyl)_2Ph_2$, $Sb(tolyl)_2Cl$ is the preferable starting material as the $Sb(tolyl)_2Li$ subsequently formed is more stable than its phenyl-substituted counterpart.

The ruthenium-antimony clusters obtained were converted to the phosphine-substituted derivatives through TMNO-mediated substitution of a carbonyl by a phosphine ligand. The reaction proceeded in moderate yield with some of the disubstituted derivative as the main side product.

*4.2 ^{1}H VT-NMR spectra of $Ru_3(CO)_9(PMe_3)(\mu\text{-}SbPh_2)_2$ (**1**)*

VT-NMR spectra of $Ru_3(CO)_9(PMe_3)(\mu\text{-}SbPh_2)_2$ (**1**) were recorded in d8-toluene from -80 ℃ to 80 ℃ (Figure 1). Unfortunately, the spectra showed no evidence of chemical exchange.

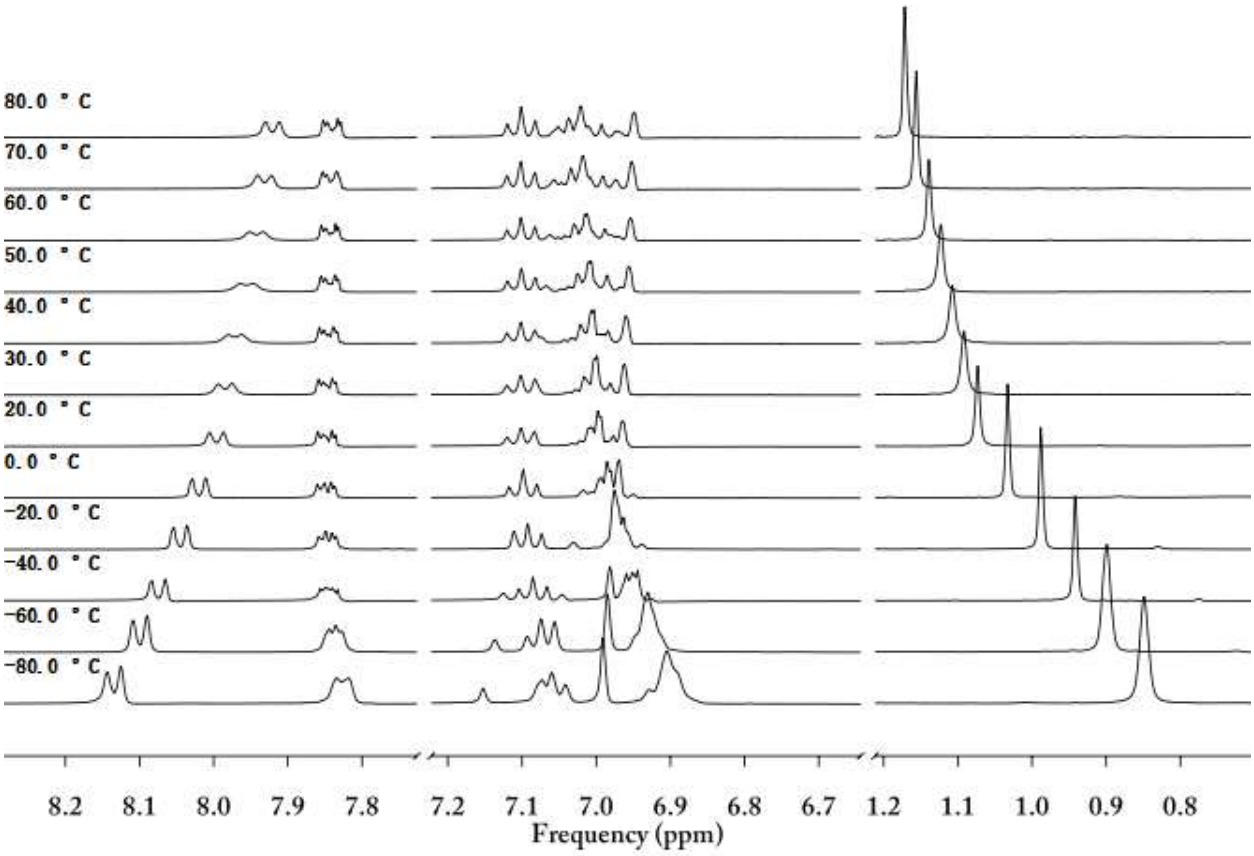

Fig. 1 $^{1}H\{^{31}P\}$ VT-NMR spectra of **1** (Solvent: toluene-d8)

A plausible explanation for this phenomenon is that the electron-donating ability of PMe_3 deviates too much from that of carbonyl ligands, making one isomer much more energetically favorable than the other. This hypothesis is consistent with the calculated activation energy of fluxional processes in **2** and **3** discussed in latter part of this report. It is also possible that the phosphine ligand, for some reason, added syn to the neighboring ruthenium, thereby sterically blocking the path by which the carbonyl ligand underwent bridge-terminal exchange. Further knowledge of molecular structure obtained from X-ray crystallography is necessary to either prove or disprove this assumption.

*4.3 ^{1}H VT-NMR spectra of $Ru_3(CO)_9(PMePh_2)(\mu\text{-}SbPh_2)_2$ (**2**) and $Ru_3(CO)_9(PPh_3)(\mu\text{-}Sb(p\text{-}tolyl)_2)_2$ (**3**)*

VT-NMR spectra of **2**, the $PMePh_2$-substituted species, were recorded in d8-toluene from -35 ℃ to 90 ℃ (Figure 2). Signals have been assigned by chemical shifts, integration and comparison with the spectrum of **1**, though a COSY experiment is inevitably required for more definitive answers.

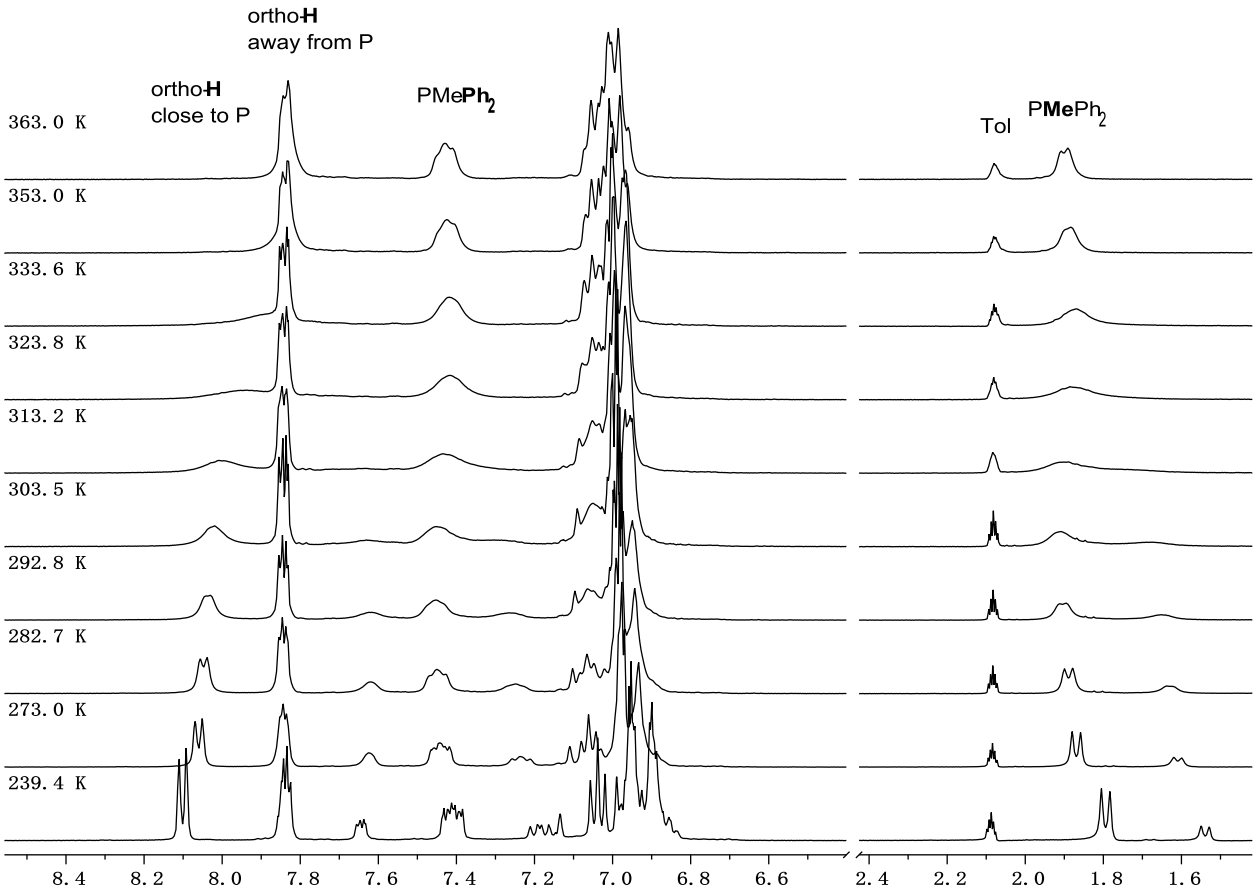

Fig. 2 ^{1}H VT-NMR spectra of **2** (Solvent: toluene-d8)

At -35 ℃, two methyl signals were observed, indicating the presence of two isomers at the low-temperature limit. On warming the sample, the two signals broadened and coalesced due to acceleration of the intramolecular chemical exchange. This observation disproves the mechanism involving phosphine migration, for in that case the chemical environment of the

phosphine ligand would remain the same before and after the exchange. The remaining two mechanisms, CO migration and the "turnstile" mechanism, are both consistent with the current available data. A carbon 2D EXSY experiment performed with ^{13}C saturated compound **2** is required to further elucidate the problem.

VT-NMR spectra of **3**, the PPh_3-substituted $Sb(p\text{-tolyl})_2$-bridged species, were recorded in d8-toluene from -40 ℃ to 80 ℃ (Figure 3). The coalescence pattern is generally similar to that of **2**; thus a similar mechanism may apply.

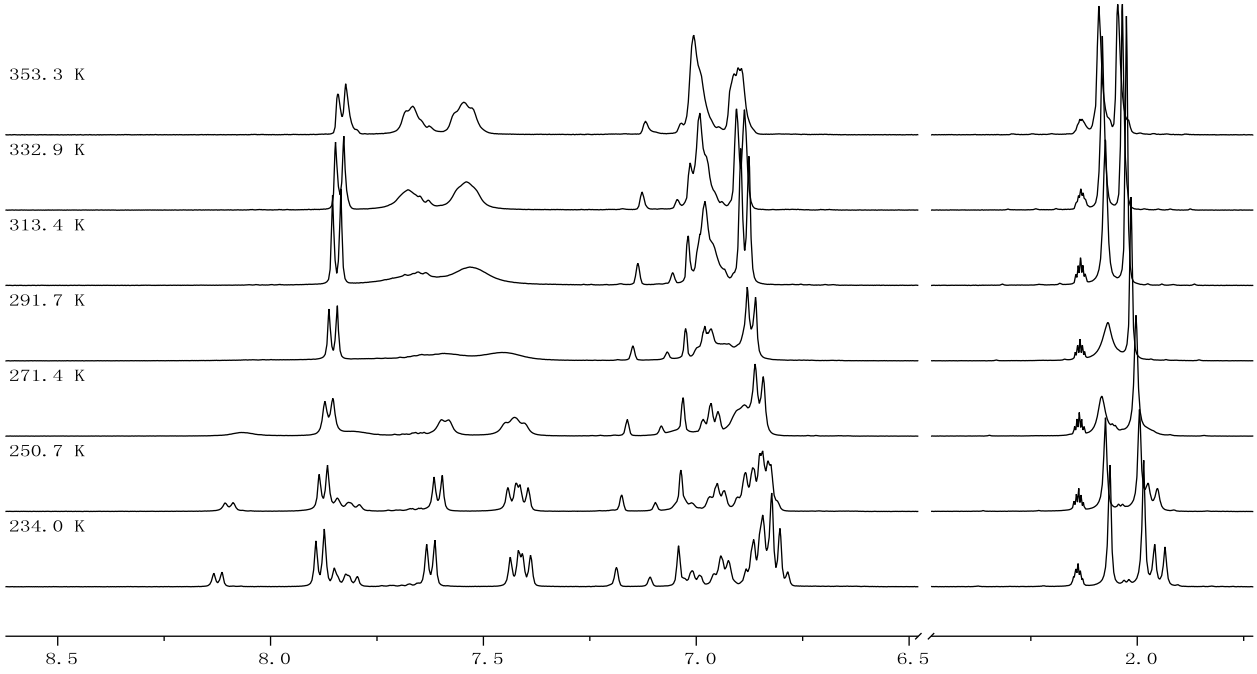

Fig. 3 ^{1}H VT-NMR spectra of **3** (Solvent: toluene-d8)

Kinetic parameters of molecular fluxionality can be estimated through lineshape analysis of ^{31}P VT-NMR spectra (Appendix I & III). An estimation of rate constants using reduced Bloch equation, combined with the plot derived from the Eyring equation (Appendix II & IV), gives entropy of activation, $\Delta S^{\neq}$, and enthalpy of activation, $\Delta H^{\neq}$ (Table 1).[6] The activation energies were derived from plotting a linear function of the Arrhenius equation (Appendix III & VI).

Table. 1 Calculated kinetic parameters for molecular fluxionality.

	Ea (kJ/mol)	$\Delta S^{\neq}$ (J/mol)	$\Delta H^{\neq}$ (kJ/mol)
2	77.1 (9)	36.6 (30)	74.7 (9)
3	58.4 (3)	-10.1 (11)	56.0 (3)

As shown in the table, the more electron-donating $PMePh_2$-substituted species **2** has considerably higher activation barrier of intramolecular chemical exchange than **3**, the less electronegative PPh_3-substituted species. Considering the fact that PMe_3-substituted cluster simply cannot undergo fluxional process in the attainable temperature range, it is inferred that the electronic property of substitutes play an important role in determining the energy barrier of this reaction.

5 Conclusion

We have shown that, among the three phosphine-substituted clusters, the PMe_3 substituted species exhibit no fluxionality in the temperature range of -80 ℃ to 80 ℃. The $PMePh_2$ and PPh_3 substituted species, on the contrary, were shown to have fluxionality with very similar coalescence patterns. The fluxional barrier of the latter molecule was calculated to be lower than the former, indicating that clusters with stronger π-accepting phosphine substitutes undergo the fluxional process more easily. The existence of two isomers at low temperature disproves the phosphine migration mechanism. Further characterization needs to be performed in order to determine the exact dynamic process that occurred.

6 Experimental

6.1 General Procedures

All reactions were carried out in an argon-filled dry box unless cooling was required, in which case standard Schlenk technique was employed. Solvents were purified and dried by distillation and kept under nitrogen prior to use. The TLC plate used was bought from a commercial supplier (silica gel 60 F254, Merck Co.). ^{1}H NMR spectra were acquired on a Bruker AV 300 spectrometer at room temperature in C_6D_6 unless otherwise stated. $SbPh_2Cl$ and $Sb(C_6H_4Me)_2Cl$ were prepared according to literature methods.[7]

6.2 Synthesis of $SbPh_2H$

To a suspension of $LiAlH_4$ (60 mg, 1.58 mmol) in ether (40 ml) was added a solution of $SbPh_2Cl$ (720 mg, 2.31 mmol) in ether (20 ml). Excessive stirring was avoided as it would hinder the sedimentation of $LiAlH_4$ in the process of purification. After 1 h of gentle stirring, the solvent was removed *in vacuo* and the mixture redissolved in hexane (20 ml). The precipitate was allowed to settle to the bottom and the supernatant was carefully transferred with a pipet into a Carius tube, followed by removal of the solvent to yield $SbPh_2H$ as a white solid (569 mg, 2.06 mmol). ^{1}H NMR δ 7.50 (m, 4 H), 7.04 (m, 6 H), 5.70 (s, 1 H);

6.3 Synthesis of Sb_2Ph_4

The $SbPh_2H$ (569 mg, 2.06 mmol) prepared as described above, was dissolved in THF (40 ml). n-Butyllithium (1.6 ml, 2.56 mmol) was added dropwise to the solution with stirring at -78 ℃ (dry ice/acetone bath). The solution turned crimson red upon addition. Subsequently, $SbPh_2Cl$ (640 mg, 2.06 mmol) was directly added to the solution. The complete consumption of the antimony-lithium compound was indicated by the change in color of the solution from red to yellow. After the reaction was completed, the solvent was removed and the precipitate recrystallized from ether at -30 ℃ to give a yellow crystalline solid (340 mg, 60%). ^{1}H NMR δ 7.55 (m, 5 H), 7.13 (comp, 10 H), 7.02 (m, 5 H);

* $Sb_2(tolyl)_4$ was prepared by exactly the same procedure from $Sb(tolyl)_2Cl$ (10%). ^1H NMR δ 7.57 (m, 8 H), 7.02 (d, 4 H), 6.91 (d, 4 H).

6.4 Synthesis of $Ru_3(CO)_{10}(\mu\text{-}SbPh_2)_2$

$Ru_3(CO)_{12}$ (255.7 mg, 0.4 mmol) and Sb_2Ph_4 (278 mg, 0.50 mmol) were stirred in THF (30 ml) to form a suspension. The mixture was cooled in a dry ice/acetone bath. Subsequently, a solution of TMNO (60 mg, 0.8mmol) in ACN (10 ml) was added dropwise over 5 min. The mixture was allowed to warm up to ~10 ℃ and stirred for 18 h, while any gas evolved was periodically removed by evacuating on the vacuum line. Removal of solvent *in vacuo* gave the crude product as an orange solid.

The crude product was dissolved in a minimum amount of dichloromethane and then transferred onto a silica gel column. Elution with hexane gave unreacted $Ru_3(CO)_{12}$. Further elution with DCM/hexane (1:1, v/v) gave the product as an orange solid (92 mg, 20%). IR(ν(CO), DCM) 2094m, 2052m, 2025s, 2020s, 1987br, 1920br.

* $Ru_3(CO)_{10}(\mu\text{-}Sb(tolyl)_2)_2$ was prepared by exactly the same procedure from $Sb_2(tolyl)_4$ and $Ru_3(CO)_{12}$ (11%). IR(ν(CO), DCM) 2093m, 2051m, 2024s, 2018sh, 1983m, 1968sh; ^1H NMR δ 7.93 (d, J = 7.5 Hz, 8 H), 6.99 (d, J = 7.7 Hz, 8 H), 2.05 (s, 12 H).

*6.5 Synthesis of $Ru_3(CO)_9(\mu\text{-}SbPh_2)_2P(CH_3)_3$ (**1**).*

$Ru_3(CO)_{10}(\mu\text{-}SbPh_2)_2$ (0.0284 g, 0.025 mmol), was dissolved in anhydrous DCM (6 ml) and cooled in an ice bath. A solution of TMNO (0.0019 g, 0.025 mmol) in anhydrous ACN (2.53 ml) was added dropwise through a pressure-equalising addition funnel, followed by dropwise addition of a solution of $P(CH_3)_3$ in toluene (3 ml of a 1M solution, 0.03 mmol). The reaction mixture was stirred for 2 h. Removal of the solvent in vacuum and separation by TLC with DCM/hexane (2:3, v/v) afforded **1** as a banana-yellow band (5.7 mg, 19%). R_f = 0.60; IR(ν(CO), DCM) 2029mw, 2002m, 1992s; ^1H NMR δ 8.08 (d, J = 6.9 Hz, 4 H), 7.89 (m, 4

H), 7.12 (d, *J* = 7.5 Hz, 4 H), 7.00 (comp, 8H), 1.02 (d, *J* = 9.2Hz, 9 H); $^{31}P\{^{1}H\}$ NMR δ -14.7s, -11.3s.

* **2** was prepared by exactly the same procedure from $Ru_3(CO)_{10}(\mu\text{-}SbPh_2)_2$ and $PMePh_2$ (38%). IR(*ν*(CO), DCM) 2055m, 2031m, 2005sh, 1993s, 1971sh, 1951sh; ^{1}H NMR *δ* 8.18 (br, 3 H), 7.99 (m, 4 H), 7.53 (br, 5 H), 7.18 (br, 4 H), 7.09 (m, 8 H), 7.05 (br, 6 H), 1.99 (br, 3 H); $^{31}P\{^{1}H\}$ NMR δ 13.6s, 8.71s.

* **3** was prepared by exactly the same procedure from $Ru_3(CO)_{10}(\mu\text{-}Sb(tolyl)_2)_2$ and PPh_3 (32%). IR(*ν*(CO), DCM) 2062w, 2033m, 2005shm 1992s, 1956sh; ^{1}H NMR *δ* 7.95 (d, 5 H), 7.79 (br, 3 H), 7.61 (br, 6 H), 6.94 (comp, 17 H), 2.11 (s, 6 H), 2.05 (s, 6 H); $^{31}P\{^{1}H\}$ NMR δ 51.8s, 30.6s.

7 References

1. Leong, W. K.; Chen, G., *J. Chem. Soc., Dalton Trans.* **2000,** *0* (23), 4442-4445
2. Li, Y.; Leong, W. K.; unpublished work
3. Bradford, A. M.; Jennings, M. C.; Puddephatt, R. J., *Organometallics* **1988,** *7* (3), 792-793.
4. Hsu, H.-F.; Shapley, J. R., *J. Organomet. Chem.* **2000,** *599* (1), 97-105.5
5. Calderazzo, F.; Poli, R.; Pelizzi, G., *J. Chem. Soc., Dalton Trans.* **1984,** *0* (11), 2365-2369.
6. Gasparro, F. P.; Kolodny, N. H., *J. Chem. Educ.* **1977,** *54* (4), 258.
7. Nunn, M.; Sowerby, D. B.; Wesolek, D. M., *J. Organomet. Chem.* **1983,** *251* (3), c45-c46.

8 Appendix

Appendix I. ^{31}P VT-NMR spectra of **2**

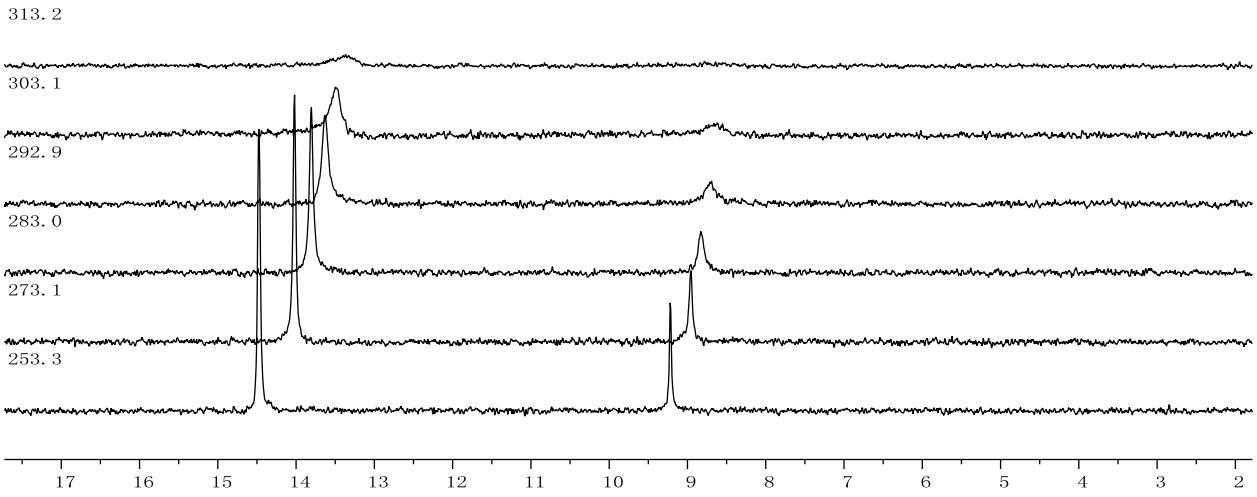

Appendix II. Eyring plot for **2**

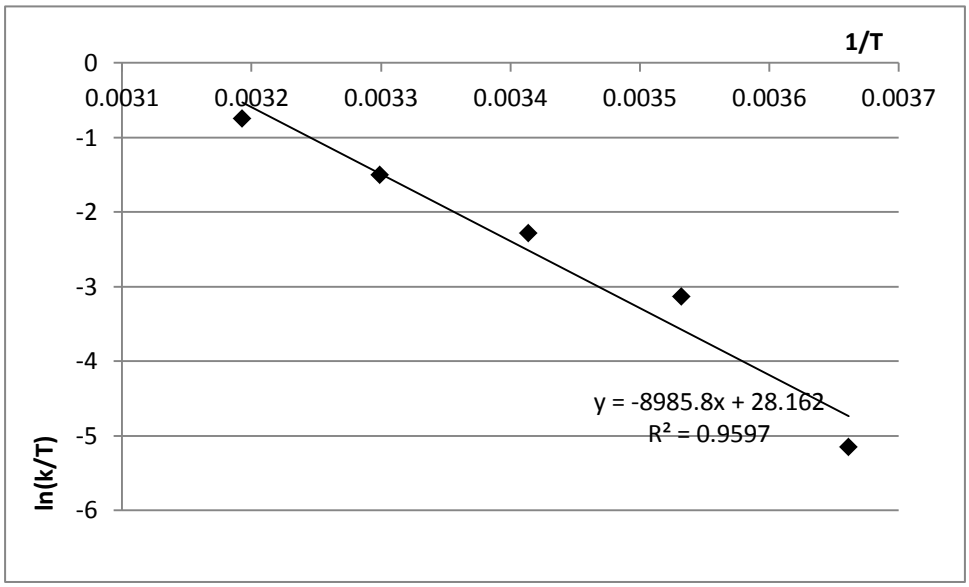

Appendix III. Arrhenius plot for **2**

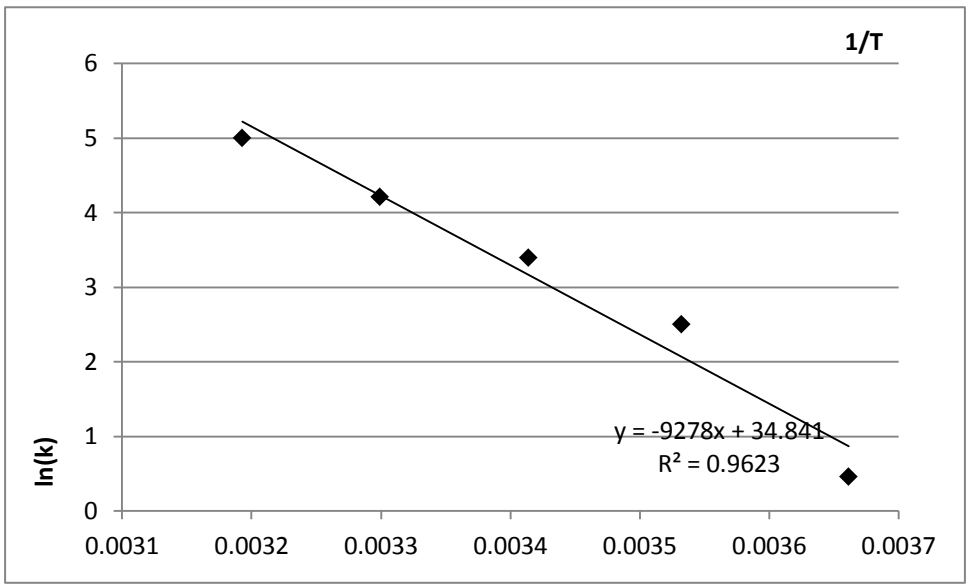

Appendix VI. ^{31}P VT-NMR spectra of **3**

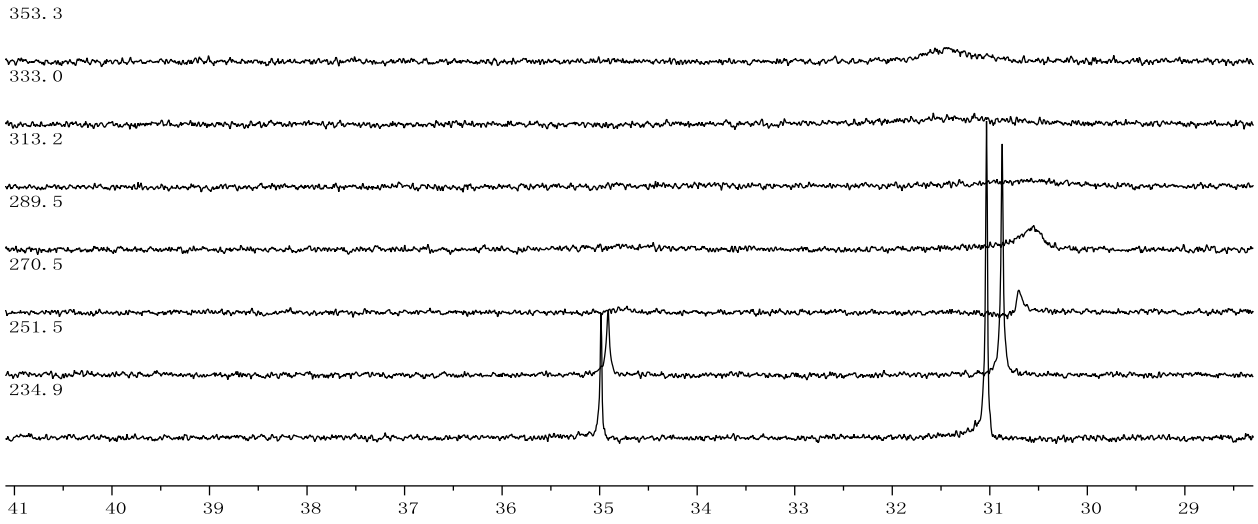

Appendix V. Eyring plot for **3**

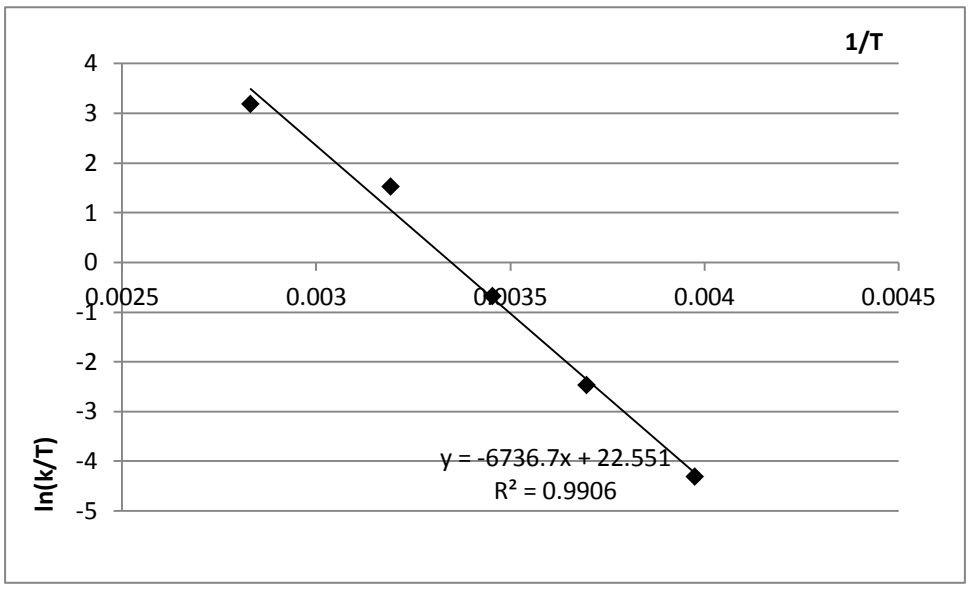

Appendix IV. Arrhenius plot of **3**